Revista Mexicana de Astronomía y Astrofísica, **49**, 127–135 (2013)

ANALYTIC AND NUMERICAL CALCULATIONS OF THE RADIAL STABILITY OF THE ISOTHERMAL SPHERE

A. C. Raga,[1] J. C. Rodríguez-Ramírez,[1] A. Rodríguez-González,[1] V. Lora,[2] and A. Esquivel[1]

Received 2012 December 3; accepted 2013 February 14

RESUMEN

Usamos una solución analítica aproximada de toda la extensión radial de una esfera no singular, isotérmica, autogravitante para derivar analíticamente las propiedades generales de las esferas resultantes, y su estabilidad a perturbaciones radiales. Derivamos el criterio de estabilidad de Bonnor y Ebert, y confirmamos analíticamente sus resultados (numéricos). Finalmente, calculamos simulaciones esféricamente simétricas de las ecuaciones de dinámica de gases Lagrangeanas, con dependencia temporal, mostrando que la transición entre soluciones estables e inestables sí ocurre en un valor del radio exterior de la esfera cercano al obtenido del criterio de estabilidad de Bonnor.

ABSTRACT

We use an approximate, analytic solution to the full radial extent of the non-singular, isothermal, self-gravitating sphere to derive analytically the general properties of the resulting spheres, and their stability to radial perturbations. We rederive the stability criterion of Bonnor and Ebert, and confirm analytically their (numerical) results. Finally, we compute spherically symmetric simulations of the time-dependent, Lagrangean, gas-dynamic equations, showing that the transition between stable and unstable solutions does occur for a value of the outer radius of the sphere close to the one obtained from Bonnor's stability criterion.

Key Words: galaxies: halos — ISM: clouds — stars: formation

1. INTRODUCTION

The study of the hydrostatic configurations of self-gravitating, isothermal spheres dates from the turn of the 19th century (see, e.g., Emden 1907). While the equation describing this equilibrium (the Lane-Emden equation) allows an analytic, singular solution, the general, non-singular solution cannot be obtained analytically (see the detailed discussion of Chandrasekhar 1967).

Bonnor (1956) and Ebert (1957) presented a radial stability analysis of the general solution of the Lane-Emden equation. Bonnor (1956) used the numerical solution tabulated by Emden (1907) to show that there is a maximum outer cloud radius beyond which an isothermal sphere is unstable to radial collapse.

More recent, approximate analytic solutions of the non-singular, isothermal sphere (Raga et al. 2013, who present an extension of the work of Hunter 2001) now allow a fully analytic calculation of Bonnor's stability criterion. We are therefore in the somewhat curious situation of being able to obtain in analytic form a derivation which was done numerically more than half a century ago.

Hunter (1977) discussed the general properties of self-gravitating, isothermal spheres, showing that for a given mass of the sphere there is a maximum possible environmental pressure beyond which an equilibrium configuration is not possible, and that there are values for this pressure for which two possible equilibrium configurations are possible. These properties now also can be derived analytically.

Finally, we feel that it is now appropriate to carry out a new numerical study of the radial collapse of isothermal spheres of sizes around Bonnor's (1956) stability limit. Numerous simulations of collapsing

[1]Instituto de Ciencias Nucleares, Universidad Nacional Autónoma de México, Mexico.

[2]Astronomisches Rechen-Institut Zentrum für Astronomie, Heidelberg, Germany.

isothermal spheres have now been made. Some examples of these are:

- Bodenheimer & Sweigart (1968): radial collapse of initially unstable spheres,
- Hunter (1977): radial collapse of spheres close to the stability limit,
- Foster & Chevalier (1993): radial collapse of the marginally stable sphere,
- Henebelle et al. (2003): radial collapse of an initially stable sphere subjected to a monotonically increasing outer pressure (3D simulations).

As far as we are aware, the paper of Hunter (1977) presents the only study of gasdynamic simulations of isothermal spheres with outer radii bracketing the stability limit. Therefore, it is interesting to re-explore this problem with the much higher resolution simulations which are now possible.

The paper is organized as follows. We give a summary of the approximate analytic solution of Lane-Emden's equation derived by Raga et al. (2013) in § 2. We then use this solution to derive the general properties of the isothermal sphere (i.e., the analysis of Hunter 1977) in § 3. We present the analytic derivation of Bonnor's (1956) stability criterion in § 4. § 5 describes numerical simulations of isothermal spheres with parameters bracketing the stability limit. Finally, the results are summarized in § 6.

2. THE NON-SINGULAR, ISOTHERMAL SPHERE SOLUTION

The non-singular solution to the isothermal, Lane-Emden equation

$$\frac{d}{dR}\left(R^2\frac{d\ln\rho}{dR}\right)=-\frac{4\pi G}{c_0^2}\rho R^2\,, \tag{1}$$

can be written in the form:

$$\rho(R)=\frac{\rho_c}{3}\left(\frac{R_c}{R}\right)^2 f\left(\frac{R}{R_c}\right)\,, \tag{2}$$

where ρ is the density as a function of spherical radius R. The core radius R_c, and the central density ρ_c satisfy the relation:

$$\rho_c=\frac{3c_0^2}{2\pi G R_c^2}\,, \tag{3}$$

where G is the gravitational constant and c_0 is the isothermal sound speed.

The Lane-Emden equation also has the singular solution:

$$\rho_s(R)=\frac{c_0^2}{2\pi G}\frac{1}{R^2}\,, \tag{4}$$

and it is common practice to consider the fractional deviation

$$q(R)=\frac{\rho(R)}{\rho_s(R)}-1 \tag{5}$$

between the non-singular (equation 2) and singular (equation 4) solutions.

Even though there is no exact analytic form for the function $f(R/R_c)$ (see equation 2), a number of approximate forms have been derived (see, e.g., Liu 1996; Natarajan & Lynden-Bell 1997, and Hunter 2001). In this paper, we use one of the approximations derived by Raga et al. (2013), which approximates the full non-singular solution (i.e., for all values of R/R_c). This approximate solution is summarized in the Appendix.

The mass within a radius R can be calculated as:

$$M(R)=4\pi\int_0^R\rho(R')R'^2dR'=\frac{2c_0^2R_c}{G}F\left(\frac{R}{R_c}\right)\,, \tag{6}$$

with

$$F\left(\frac{R}{R_c}\right)=\int_0^{R/R_c}f(r)dr\,. \tag{7}$$

This function can be calculated analytically from the approximate solution of Raga et al. (2013), as discussed in the Appendix.

3. MAXIMUM MASS AND RADIUS OF AN ISOTHERMAL SPHERE

Let us consider a self-gravitating sphere of isothermal sound speed c_0 embedded in an environment of pressure $\rho_e c_0^2$ (so that the outer density of the sphere has a value ρ_e). From equation (2) we can then obtain the outer radius R_e of the sphere:

$$R_e=\sqrt{\frac{c_0^2}{2\pi G\rho_e}f(r_e)}\,, \tag{8}$$

and from equation (6) the total mass:

$$M=\frac{2c_0^3}{\sqrt{2\pi\rho_e G^3}}\frac{f^{1/2}(r_e)F(r_e)}{r_e}\,, \tag{9}$$

as a function of the ratio $r_e=R_e/R_c$ between the external radius and the core radius of the sphere.

The outer radius and total mass of the sphere (equations 8 and 9) are plotted as a function of R_e/R_c in Figure 1. In this figure, we see that for a sphere with weak gravity (i.e., with $R_c\gg R_e$) we

naturally obtain $R_e \propto R_e/R_c$ and $M \propto (R_e/R_c)^3$, as would be expected for a sphere with an approximately uniform density (with a value $\approx\rho_e$).

From Figure 1 we also see that for $R_e/R_c \gg 1$, the outer radius and the total mass reach asymptotic values R_a and M_a (respectively), with values

$$R_a = \sqrt{\frac{c_0^2}{2\pi G\rho_e}}\,, \tag{10}$$

$$M_a = \frac{2c_0^3}{\sqrt{2\pi\rho_e G^3}}\,, \tag{11}$$

corresponding to the radius and mass of the singular isothermal sphere solution (equation 4). These values can be obtained from equations (8) and (9) by setting $f(r_e) = 1$ and $F(r_e) = r_e$.

From Figure 1, we see that the outer radius of the sphere has a maximum value $R_m = 1.289R_a$ (obtained for $R_e/R_c = 1.661$) and the mass has a maximum possible value $M_m = 1.918M_a$ (obtained for $R_e/R_c = 9.034$). Therefore, the maximum possible radius is ≈30% larger than the one of the singular sphere, and the maximum possible mass is ≈90% larger than the one of the singular sphere.

In the top frame of Figure 1 we also see that for $M > M_a$ (corresponding to $R > 2.646\,R_c$) there are two isothermal sphere solutions (with mass M and external density ρ_e) with different radii. The existence of these two possible solutions was noted by Hunter (1977).

In the bottom frame of Figure 1 we see that for external radii $R_e \approx R_a$ (see equation 10) two or more isothermal spheres with the same R_e and ρ_e but with different M can be constructed. Actually, in the $R_e \to R_a$ limit an infinite number of spheres (sharing the same values of R_e and ρ_e) exist, with masses which all tend to M_a (and hence differ from each other infinitesimally). These spheres, however, have significantly different values of their core radii (and hence, different R_e/R_c values, see the bottom plot of Figure 1).

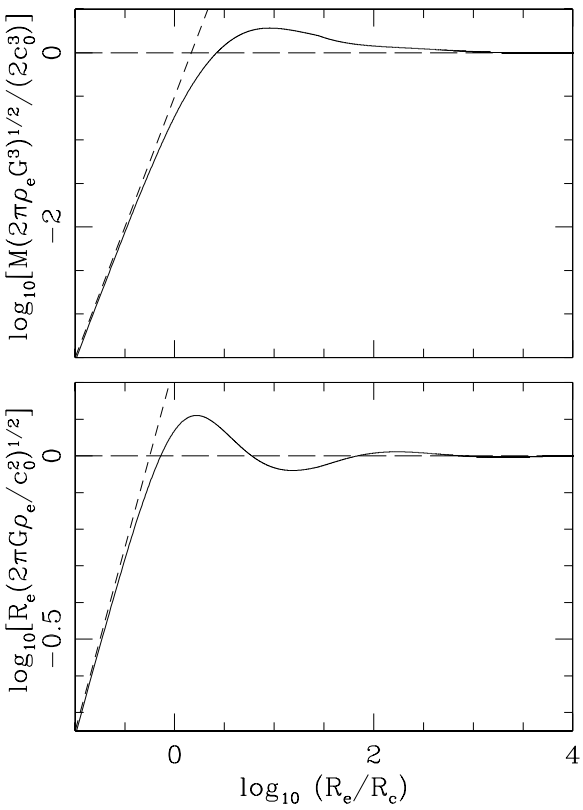

Fig. 1. Dimensionless mass (top) and outer radius (bottom) of a non-singular isothermal sphere as a function of the outer to core radius ratio R_e/R_c (solid lines). The long dash, horizontal lines represent the values obtained for the singular sphere. The short dash lines represent a $M \propto (R_e/R_c)^3$ (top graph) and a $R_e \propto R_e/R_c$ dependence (bottom).

4. BONNOR'S STABILITY ANALYSIS

Bonnor (1956) suggested the following stability criterion for radial perturbations of an isothermal sphere. If we have a sphere of total mass M and external radius R_e, it is gravitationally stable provided that

$$\left(\frac{dP_e}{dR_e}\right)_{M=\text{const.}} = c_0^2\left(\frac{d\rho_e}{dR_e}\right)_{M=\text{const.}} < 0\,, \tag{12}$$

where P_e is the outer pressure of the sphere and ρ_e its outer density (obtained by setting $R = R_e$ in equation 2). In other words, the self-gravitating sphere is stable if it can react to an increase in the pressure of the surrounding environment by generating a new hydrostatic structure with a smaller external radius.

Bonnor (1956) used a tabulation of the density stratification of the isothermal sphere of Emden (1907) in order to evaluate numerically the radial dependence of ρ_e as a function of R_e (actually, as a function of the volume $4\pi R_e^3/3$ of the sphere) at constant M. Interestingly, the more recent approximate analytic solutions of the full non-singular isothermal sphere solution (Raga et al. 2013) now allow us to obtain an analytic evaluation of the stability criterion (equation 12). This can be done as follows.

First, differentiating equation (6) we obtain:

$$\frac{G}{2c_0^2}dM = \left[F(r_e) + R_c\frac{dF}{dr_e}(r_e)\frac{\partial r_e}{\partial R_c}\right]dR_c + R_c\frac{dF}{dr_e}(r_e)\frac{\partial r_e}{\partial R_e}dR_e\,, \tag{13}$$

where $r_e = R_e/R_c$. In this equation, $\partial F/\partial r_e = f(r_e)$, $\partial r_e/\partial R_c = -R_e/R_c^2$ and $\partial r_e/\partial R_e = 1/R_c$. Setting $dM = 0$ in equation (13) we then have:

$$\frac{dR_c}{dR_e} = \frac{1}{r_e - F(r_e)/f(r_e)}\,, \tag{14}$$

for a variation at constant M.

We now evaluate equation (2) at the external radius R_e and differentiate to obtain:

$$\frac{2\pi G}{c_0^2}\frac{d\rho}{dR_e} = \frac{1}{R_e^2}\left[-\frac{2}{R_e}f(r_e) + \frac{df}{dr_e}\frac{dr_e}{dR_e}\right]\,, \tag{15}$$

where

$$\frac{dr_e}{dR_e} = \frac{1}{R_c} - \frac{R_e}{R_c^2}\frac{dR_c}{dR_e}\,. \tag{16}$$

Finally, combining equations (14–16) we obtain

$$\frac{2\pi G}{c_0^2}\frac{d\rho}{dR_e} = \frac{1}{R_e^3}\left[\frac{r_e f'(r_e)}{1 - r_e f(r_e)/F(r_e)} - 2f(r_e)\right]\,, \tag{17}$$

where $f(r_e)$ (see equation 2), $F(r_e)$ (equation 7) and $f' = df(r_e)/dr_e$ are obtained from the approximate analytic solution of Raga et al. (2013), as described in the Appendix.

Figure 2 shows the fractional deviation q between the non-singular and singular solutions (equation 5), and the appropriately dimensionless values of $|d\rho/dR_e|$ and $R_e^3\, d\rho/dR_e$ obtained from equation (17) and from the numerical non-singular solution. The results obtained from the approximate, analytic and the numerical isothermal sphere solutions are basically indistinguishable.

From the two lower plots of Figure 2 we see that $d\rho/dR < 0$ for small radii, and that $d\rho/dR = 0$ for a radius $R_s = 2.633\, R_c$. This value agrees numerically with the value obtained by Bonnor (1956) and Hunter (1977), who used a different definition of the core radius R_c (smaller than the one of equation 28 by a factor of $1/\sqrt{6}$).

For $R_s < R < 3.672\, R_c$ we have $d\rho/dR > 0$ (and, hence, an unstable behavior, see equation 12), and at larger radii we have an approximately logarithmically periodical repetition of radial bands of stable (i.e., negative $d\rho/dR$) and unstable (positive $d\rho/dR$) behavior, following the periodical crossings in $\ln R$ between the non-singular and singular solutions of the asymptotic, large R regime (seen in the top graph of Figure 2 and in equation 31 of the Appendix).

Bonnor (1956) argued that all of the isothermal spheres with $R > R_s$ are unstable (regardless of whether their outer radius R is within one of the stable or unstable outer bands). The argument is that a perturbation at the outer radius will propagate inwards, eventually reaching one of the unstable radial bands. Once one of these unstable bands has been reached, the inner part of the sphere will collapse, leading to a later collapse of the outer regions (which have lost inner support). We explore this effect numerically in § 5.

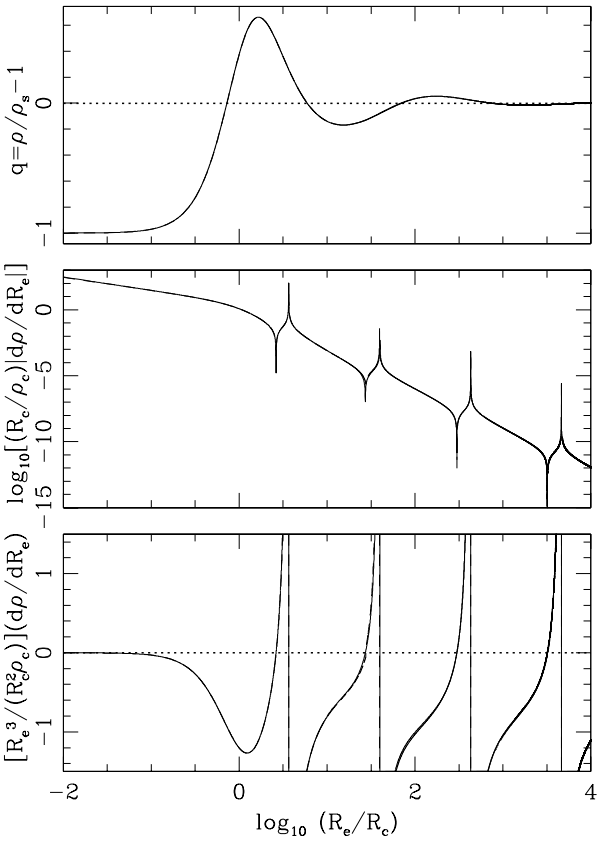

Fig. 2. Fractional deviation q between the non-singular and the singular solutions (top), and dimensionless forms of $|d\rho/dR_e|$ (centre) and $R_e^3 d\rho/dR_e$ (bottom) as a function of R_e/R_c. The values derived from the approximate analytic solution (shown with solid lines), and the values obtained from the numerical non-singular solution (shown with dashed lines) are basically indistinguishable.

We are then in the situation of being able to obtain the Jeans mass of a self-gravitating isothermal sphere embedded in an environment of pressure P_e. The density at the outer boundary of the sphere then is $\rho_e = P_e/c_0^2$.

The maximum possible mass for stability is obtained setting $R_e = R_s = 2.633\, R_c$ in equations (6), obtaining

$$M_s = \frac{2c_0^2 R_c}{G}F(2.633) = 1.634\frac{c_0^2 R_s}{G}\,, \tag{18}$$

where for the second equality we have used the fact that $F(2.633) = 2.151$ (see equation 36).

Using equation (2), we can write M_s in terms of the density ρ_e at the edge of the sphere:

$$M_s = 2\pi R_s^3 \rho_e \frac{F(2.633)}{f(2.633)} = 9.120\, R_s^3 \rho_e\,. \qquad (19)$$

In other words, the maximum mass for radial stability of the isothermal sphere is only 2.177 times the mass of a uniform sphere of density ρ_e.

5. NUMERICAL SIMULATIONS

In order to check the accuracy of Bonnor's stability criterion (equations 12, 17) we consider an initial hydrostatic, self-gravitating isothermal sphere and then numerically integrate the spherically symmetric, Lagrangean gasdynamic equations written in the form:

$$\frac{\partial}{\partial t'}\left(\frac{1}{\rho'}\right) - \frac{\partial r^2 u}{\partial m} = 0\,, \qquad (20)$$

$$\frac{\partial u'}{\partial t'} + r^2 \frac{\partial}{\partial m}\left[\rho' - \rho'_h(r_0)\right] = 6m\left[\frac{1}{r^2} - \frac{r^2}{r_0^4(m)}\right], \qquad (21)$$

with dimensionless variables are defined as

$$u' = u/c_0\,,\;\; r = R/R_c\,,\;\; t' = tc_0/R_c\,,\;\; \rho' = \rho/\rho_c\,, \qquad (22)$$

where u is the (radial) flow velocity, R the spherical radius, t the time and ρ the density of the flow, and c_0 the isothermal sound speed, R_c the core radius and ρ_c the central density of the initial isothermal sphere.

The dimensionless mass coordinate m (in equation 21) is defined as:

$$m \equiv \frac{1}{\rho_c R_c^3}\int_0^R \rho R^2\, dR\,. \qquad (23)$$

Finally $r_0(m)$ is the initial radius of the fluid parcels as a function of the mass coordinate m, and $\rho_h(r)$ is the initial hydrostatic solution (obtained from equation 2).

These equations of motion are then integrated forward in time with a simple, MacCormack finite difference method, preserving in an exact way the initial, hydrostatic solution. In order to obtain a time-dependence, we perturb the density at the outer boundary of the sphere.

We compute a set of models, for which we choose different values of the external radius $R_e = r_e R_c$ of the initial isothermal sphere, and impose a perturbed density $\rho_e + \Delta\rho_e$ (where $\rho_e = \rho_h(R_e)$ is the outer density of the hydrostatic solution given by equation 2) at the outer boundary. The initially hydrostatic sphere (except at the outer boundary, see above) is divided into N unequal mass cells, distributed so that they all have an initial $\Delta R = R_e/N$ spatial thickness. The models that we have computed have $N = 1000$ or 2000 mass cells (see Table 1).

TABLE 1

RADIAL COLLAPSE MODELS

Model	R_e/R_c [a]	$\frac{\Delta\rho_e}{\rho_e}$ [b]	$\frac{c_0 t_{\rm con}}{R_c}$ [c]	$\frac{c_0 t_{\rm coll}}{R_c}$ [d]	N [e]
C2.5	2.5	$+10^{-3}$	···	···	1000
E2.5	2.5	-10^{-3}	···	···	1000
C2.7	2.7	$+10^{-3}$	20.1	21.6	1000
E2.7	2.7	-10^{-3}	···	···	1000
C2.9	2.9	$+10^{-3}$	17.1	18.0	1000
E2.9	2.9	-10^{-3}	56.4	57.5	1000
C10	10.0	$+10^{-3}$	20.0	28.1	2000
E10	10.0	-10^{-3}	88.8	98.8	2000
C100	100.0	$+10^{-3}$	39.1	170.7	2000
E100	100.0	-10^{-3}	39.1	172.4	2000

[a]Initial radius R_e in units of the core radius R_c.

[b]Fractional density perturbation at the outer radius.

[c]Time $t_{\rm con}$ at which the central condensation starts to form.

[d]Time $t_{\rm coll}$ at which all of the sphere has collapsed.

[e]Number of radial cells in the simulation.

We have chosen the five values for the initial outer radius R_e of the sphere given in the second column of Table 1. The first three values of R_e straddle the $R_s = 2.633\, R_c$ maximum radius of Bonnor's stability criterion (see § 4). The fourth value is $R_e = 10\, R_c$, falling in the first of the radial "stability bands" (see the bottom plot of Figure 2). The fifth value is $R_e = 100\, R_c$, falling in the second of the stability bands of Bonnor's criterion.

For each of the chosen initial radii R_e of the sphere, we have computed two models, with $\Delta\rho_e = \pm 10^{-3}\rho_e$ (see Table 1). In other words, the density (or pressure) of the outer boundary of the initial, hydrostatic sphere is perturbed with a fractional change of $\pm 0.1\%$. This perturbation is maintained throughout the computed time evolution of the flow.

Figure 3 shows the density stratifications in the (t, R)-plane of the models of Table 1. Models C2.5 and E2.5, both with initial radii $R_e = 2.5R_c < R_s$, show an undamped, oscillatory time-evolution (top panels of Figure 3). For an initial radius $R_e = 2.7R_c$, slightly above the $R_s = 2.633\, R_c$ Bonnor's stabil-

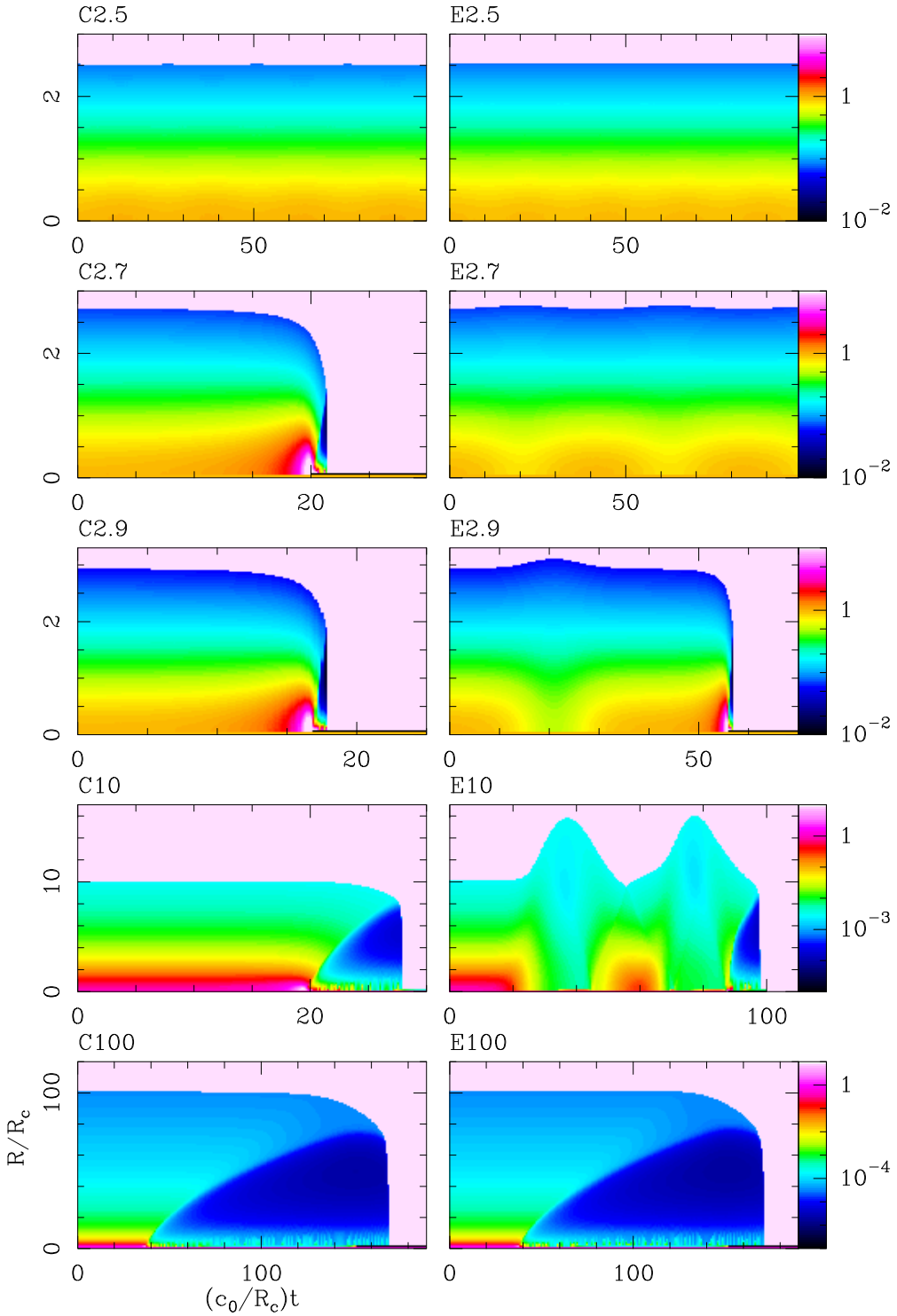

Fig. 3. Density stratifications in the (t, R)-plane obtained from the numerical models given in Table 1. The models with positive density perturbations at the outer boundary are in the left column, and the ones with negative perturbations in the right one. The dimensionless densities of the models with different values of R_e/R_c are shown with the logarithmic colour scheme given by the bars on the right. In all of the plots, the lighter regions with large R are external to the outer radius of the sphere. The color figure can be viewed online.

ity radius, we obtain a collapsing solution for a $\Delta\rho_e = 10^{-3}\rho_e$ perturbation, and an oscillatory solution for the $\Delta\rho_e = -10^{-3}\rho_e$ perturbation (models C2.7 and E2.7, respectively, see Table 1 and Figure 3). For a larger, $R_e = 2.9R_c$ initial radius we obtain collapsing solutions for both positive and negative density perturbations in the outer boundary (models C2.9 and E2.9).

Finally, for the models with initial radii $R_e = 10R_c$ and $100R_c$ (four bottom frames of Figure 3), we obtain collapsing solutions for both positive and negative density perturbations in the outer boundary, even though these initial radii have been chosen so as to lie in the outer stability bands of Bonnor's criterion (see Figure 2). The fact that these models collapse confirms Bonnor's argument that all spheres with $R_e > R_s$ ($= 2.633\,R_c$, see § 3) are unstable.

From this, we conclude that the $R_s = 2.633\,R_c$ maximum radius for stability obtained from Bonnor's criterion does represent the approximate maximum radius for stability to small radial perturbations at the outer boundary of the isothermal sphere. However, the precise value of the maximum radius appears to depend on whether the density (or pressure) perturbations are positive or negative (with a slightly larger stability radius for negative perturbations).

In all collapsing solutions there is an initial regime in which perturbations travel inwards and outwards over all of the spherical cloud. At some point, a condensed inner core is formed, and the remaining part of the evolution is a collapse of the outer material onto this core. From the simulations, we then compute two characteristic times:

- $t_{\rm con}$, at which the condensed core first starts to form,
- $t_{\rm coll}$, at which all of the material of the sphere collapses into the central condensation.

These times are given in the 4th and 5th columns of Table 1. It is clear that for larger values of the initial radius R_e, these two times become significantly different, so that the central core is present during a substantial part of the time-evolution of the collapsing sphere.

6. CONCLUSIONS

We have used the analytic approximation of the non-singular isothermal sphere of Raga et al. (2013) to explore the total mass/external radius configurations which are possible for external media of different pressures (i.e., for different outer densities of the isothermal spheres, see §§ 2 and 3). We reproduce the results of Hunter (1977, obtained numerically), who noted that for some values of the environmental pressure it is possible to have two isothermal sphere configurations with the same mass. We also note that for special values of the environmental pressure one can have a large number of isothermal spheres with the same outer radius and with very similar masses, but with substantially different values of the core radius. Finally, we note that for given values of the isothermal sound speed c_0 and outer density ρ_e, the maximum possible mass of an isothermal sphere is ≈2 times higher than the mass M_a of the singular solution (see equation 11). This maximum mass is obtained for a ratio $R_e/R_c = 9.034$ between the outer radius and the core radius of the sphere.

In the context of molecular cloud cores, for a singular isothermal sphere of outer, molecular number density $n_{\rm mol} = \rho_e/m$ (where $m \approx 2m_H$ is the mass per molecule) from equations (10–11) we obtain an outer radius and a mass:

$$R_a \approx 0.056\,{\rm pc}\,\left(\frac{T}{10\,{\rm K}}\right)^{1/2}\left(\frac{10^4{\rm cm}^{-3}}{n_{\rm mol}}\right)^{1/2}\,, \quad (24)$$

$$M_a \approx 1.1\;M_\odot\,\left(\frac{T}{10\,{\rm K}}\right)^{3/2}\left(\frac{10^4{\rm cm}^{-3}}{n_{\rm mol}}\right)^{1/2}\,, \quad (25)$$

where we have set $c_0 \approx \sqrt{kT/(2m_H)}$. These equations can be combined to obtain a "mass-radius" relation:

$$M_a \approx 2.0\;M_\odot\,\left(\frac{R_a}{0.1\;{\rm pc}}\right)\left(\frac{T}{10\;{\rm K}}\right)\,. \quad (26)$$

The mass M_m and radius R_m of the maximum mass sphere (i.e., the sphere with an external to core radius ratio $R_m/R_c = 9.034$, see above and § 3) follow a similar mass-radius relation (see equation 26), but with a leading constant of 3.0 $M_\odot$. These numbers agree with the physical scales of molecular cores in regions of low mass star formation.

We have then rederived analytically Bonnor's (1956) stability criterion for radial perturbations of an isothermal sphere (§ 4). We find that the results obtained from the analytic derivation are basically indistinguishable from the ones obtained from an numerical solution of Lane-Emden's equation, as shown in Figure 2. In particular, we find that the maximum external radius of a stable isothermal sphere is $R_s = 2.633\,R_c$, which coincides with the value found by Bonnor (1956) and with the more precise value found by Hunter (1977), noting that Bonnor and Hunter defined a core radius smaller by a factor of $1/\sqrt{6}$ with respect to the one used in the present

paper (see equation 28). The mass of this "maximal sphere" is 2.177 times larger than the mass of a uniform sphere of radius R_s, in pressure balance with the surrounding environment (see equation 19).

Finally, we computed spherically symmetric numerical simulations of isothermal spheres with different values of the external to core radius ratio R_e/R_c (see § 5). These simulations were carried out with the Lagreangean gasdynamic equations written in a form that preserves the initial hydrostatic equilibrium in an exact way. We find that imposing small, time-independent density perturbations at the outer radius of the sphere we obtain oscillating solutions for smaller values of R_e/R_c and collapsing solutions for larger R_e/R_c values. The transition between the oscillating and collapsing solutions occurs for initial external radii within ≈10% of Bonnor's (1956) stability radius, regardless of the sign of the density perturbation at the outer radius. We also show that isothermal spheres with radii $R_e > R_s$ within the outer stability bands of Bonnor's criterion are also unstable (as predicted by Bonnor 1956).

Even though Hunter (1977) computed simulations of isothermal spheres close to the stability limit, he does not say whether or not his simulations confirm the transition to collapsing solutions for $R_e > R_s$. Hunter mentions that in some unstable simulations with R_e "well in excess" of R_s he fails to obtain collapsing solutions due to the fact that his numerical integration does not preserve with enough precision the initial hydrostatic configuration. Our simulations avoid this problem by solving a set of equations which automatically preserves the initial equilibrium.

The time-evolution obtained from our simulations is similar to the ones of Hunter (1977) or to more recent calculations like the ones of Foster & Chevalier (1993) and Hennebelle et al. (2003). These authors compare their solutions with self-similar collapse solutions (see, e.g., Larson 1969 and Penston 1969) and with observations of molecular cloud cores. We have not carried out such comparisons.

We end our discussion by noting that the maximum stable radius $R_s = 2.633\,R_c$ obtained from Bonnor's (1956) radial stability analysis does not necessarily correspond to the maximum possible radius of stable molecular cloud cores. One of the possible caveats is that it is highly unlikely to have a coordinated radial perturbation which will lead to a collapse giving rise to the formation of a core at the precise center of the configuration. Perturbations with a strong asymmetry (which are more easily imaginable in an astrophysical context, see, e.g., Esquivel & Raga 2007) will be less efficient in producing a collapse.

Another possible effect is that the presence of a finite timescale for reaching thermal equilibrium will produce deviations from a precisely isothermal behavior. We will explore the effect of a finite thermal timescale on the stability of isothermal spheres in a future paper.

Finally, we should note that Bonnor's (1956) stability analysis is not applicable for isothermal sphere configurations in the context of N-body systems, which react adiabatically to external perturbations. The stability analysis of Lynden-Bell & Wood (1968) is more relevant for such systems.

We acknowledge support from the Conacyt grants 61547, 101356, 101975, 165584 and 167611, and the DGAPA-Universidad Nacional Autónoma de México grants IN105312 and IN106212. We thank an anonymous referee for several sugestions (out of which arose the discussion at the end of § 4, with equations 18 and 19, and to equations 24–26 in § 6).

APPENDIX. THE NON-SINGULAR SOLUTION

We consider the second approximation for the full, non-singular isothermal sphere proposed in § 6 of Raga et al. (2013). This solution has a density stratification which can written in the form:

$$\rho(R) = \frac{c_0^2}{2\pi G R^2}\, f\left(\frac{R}{R_c}\right) , \tag{27}$$

where R is the spherical radius, G the gravitational constant, c_0 the isothermal sound speed,

$$R_c = \sqrt{\frac{3c_0^2}{2\pi G \rho_c}} , \tag{28}$$

is the core radius and ρ_c the central density.

The $f(r)$ function (with $r = R/R_c$) is approximated by a "near" and a "far field" interpolation ($f_{\rm near}$ and $f_{\rm far}$, respectively), with a switch at a radius $r_1 = 27.643$:

$$f(r) = f_{\rm near}(r)\,, r \le r_1\,; \quad f(r) = f_{\rm far}(r)\,, r > r_1\,, \tag{29}$$

with

$$f_{\rm near}(r) = \sum_{j=1}^{4} \frac{A_j}{2 + a_j^2/(3r^2)} , \tag{30}$$

and

$$f_{\rm far}(r) = 1 + \frac{A}{r^{1/2}}\,\cos\left(\frac{\sqrt{7}}{2}\ln r + \phi\right)\,, \qquad (31)$$

where $A = 0.735$, $\phi = 5.396$ and the values of A_j and a_j given in Table 2 of Hunter (2001).

With these forms for $f_{\rm near}(r)$ and $f_{\rm far}(r)$ it is straightforward to calculate the derivative $f'(r)$ of f with respect to r:

$$f'(r) = f'_{\rm near}(r)\,, r \le r_1\,;$$

$$f'(r) = f'_{\rm far}(r)\,, r > r_1\,, \qquad (32)$$

with

$$f'_{\rm near}(r) = \frac{2}{3}\sum_{j=1}^{4}\frac{a_j^2 A_j r}{(2r^2 + a_j^2/3)^2}\,, \qquad (33)$$

and

$$f'_{\rm far}(r) = -\frac{A}{2r^{3/2}}\left[\sqrt{7}\sin\left(\frac{\sqrt{7}}{2}\ln r + \phi\right) + \cos\left(\frac{\sqrt{7}}{2}\ln r + \phi\right)\right]. \qquad (34)$$

We can also calculate the integral

$$F(r) = \int_0^r f(r')dr' \qquad (35)$$

as

$$F(r) = I_1(r)\,, r \le r_1\,;$$

$$F(r) = I_1(r_1) + I_2(r) - I_2(r_1)\,, r > r_1\,, \qquad (36)$$

where

$$I_1(r) = \sum_{j=1}^{4}\frac{A_j}{2}\left[r - \frac{a_j}{\sqrt{6}}\tan^{-1}\left(\frac{\sqrt{6}r}{a_j}\right)\right], \qquad (37)$$

$$I_2(r) = r + \frac{Ar^{1/2}}{4}\left[\sqrt{7}\sin\left(\frac{\sqrt{7}}{2}\ln r + \phi\right) + \cos\left(\frac{\sqrt{7}}{2}\ln r + \phi\right)\right]. \qquad (38)$$

REFERENCES

Chandrasekhar, S. 1967, An Introduction to the Study of Stellar Structure (New York: Dover)
Bodenheimer, P., & Sweigart, A. 1968, ApJ, 152, 515
Bonnor, W. B. 1956, MNRAS, 116, 351
Ebert, R. 1957, Zert. Astrophys., 42, 263
Emden, R. 1907, Gaskugeln (Leipzig: Teubner)
Esquivel, A., & Raga, A. C. 2007, MNRAS, 377, 383
Foster, P. N., & Chevalier, R. A. 1993, ApJ, 416, 303
Hennebelle, P., Whitworth, A. P., Gladwin, P. P., & André, Ph. 2003, MNRAS, 340, 870
Hunter, C. 1977, ApJ, 218, 834
_____. 2001, MNRAS, 328, 839
Larson, R. B. 1969, MNRAS, 145, 271
Liu, F. K. 1996, MNRAS, 281, 1197
Lynden-Bell, D., & Wood, R. 1968, MNRAS, 138, 495
Natarajan, P., & Lynden-Bell, D. 1997, MNRAS, 286, 268
Penston, M. V. 1969, MNRAS, 144, 425
Raga, A. C., Rodríguez-Ramírez, J. C., Villasante, M., Rodríguez-González, A., & Lora, V. 2013, RevMexAA, 49, 63

A. C. Raga, J. C. Rodríguez-Ramírez, A. Rodríguez-González, and A. Esquivel: Instituto de Ciencias Nucleares, Universidad Nacional Autónoma de México, Apdo. Postal 70-543, 04510 D.F., Mexico (raga, juan.rodriguez, ary@nucleares.unam.mx).

V. Lora: Astronomisches Rechen-Institut Zentrum für Astronomie der Universität Heidelberg, Mönchhofstr. 12-14, 69120 Heidelberg, Germany (verolora@gmail.com).